

A New Nonfullerene Acceptor with Near Infrared Absorption for High Performance Ternary-Blend Organic Solar Cells with Efficiency over 13%

Huan-Huan Gao, Yanna Sun, Xiangjian Wan,* Xin Ke, Huanran Feng, Bin Kan, Yanbo Wang, Yamin Zhang, Chenxi Li, and Yongsheng Chen*

A new acceptor–donor–acceptor (A–D–A) type nonfullerene acceptor, 3TT-FIC, which has three fused thieno[3,2-*b*]thiophene as the central core and difluoro substituted indanone as the end groups, is designed and synthesized. 3TT-FIC exhibits broad and strong absorption with extended onset absorption to 995 nm and a low optical bandgap of 1.25 eV. The binary device based on 3TT-FIC and the polymer PTB7-Th exhibits a power conversion efficiency (PCE) of 12.21% with a high short circuit current density (J_{sc}) of 25.89 mA cm⁻². To fine-tune the morphology and make full use of the visible region sunlight, phenyl-C₇₁-butyricacid-methyl ester (PC₇₁BM) is used as the third component to fabricate ternary devices. In contrast to the binary devices, the ternary blend organic solar cells show significantly enhanced EQE ranging from 300 to 700 nm and thus an improved J_{sc} with a high value of 27.73 mA cm⁻². A high PCE with a value of 13.54% is achieved for the ternary devices, which is one of the highest efficiencies in single junction organic solar cells reported to date. The results provide valuable insight for the ternary devices in which the external quantum efficiency (EQE) induced by the third component is evidently observed and directly contributed to the enhancement of the device efficiency.

In the past decades, organic solar cells (OSCs) have drawn extensive attentions due to their advantages such as low cost and large area printing production, flexibility, semitransparency, etc.^[1–6] Presently, OSCs in labs have made significant progress with power conversion efficiency (PCE) over 13% for single junction devices,^[7] mainly due to new active materials development and device optimizations.^[8–11] Despite the


great success for the fullerene-based OSCs in earlier years,^[12–14] the dominated acceptor materials, fullerene derivatives, have some intrinsic drawbacks such as weak absorption, poor chemical and electronic adjustability, etc., limiting the further improvement of the photovoltaic performance. To address those issues and further improve OSCs efficiencies, great attentions have been paid to develop nonfullerene acceptors (NFAs) with wide and tunable absorption windows, easily tuned energy levels.^[15–17] In just recent years, NFAs-based OSCs have made significant progress with breakthrough PCEs over 13% for single junction devices.^[7] On the other hand, besides exploring the device optimization methods such as thermal and solvent annealing, additive, etc., the device structures such as tandem^[18–20] and ternary devices^[21–24] have also been explored intensively in order to further improve the performance. In contrast

to the complicated fabrication process of tandem structure OSCs, ternary devices with three components (two donors with one acceptor or one donor with two acceptors) have a simpler process to fabricate devices. Furthermore, it can also take the advantage of tandem devices with enhanced photon harvesting by incorporating the third component.^[25–29]

In ternary devices, the additional component usually exhibits complementary absorption with the binary materials. Also it needs to have suitable energy levels to offer enough driving forces for exciton dissociation and charge extraction.^[21,30] This is because such a cascade energy structure would bridge the donor and acceptor energy offset and facilitate exciton dissociation and then improve the open-circuit voltage (V_{oc}).^[25,31,32] In recent years, great progress has been made for the ternary OSCs, including new materials design, morphology optimization, and mechanism understanding.^[30,33] Just recently, PCEs over 14% have been reported by Ding and co-workers^[22] with a ternary device using a low band gap NFA acceptor, demonstrating great potential of ternary devices.

Recently, our^[34] and other groups^[2,35] have almost simultaneously reported an A–D–A NFA TTIC with a broad and near infrared absorption ranging from 600 to 900 nm in the thin film. PCE of 10.87% was achieved when polymer PBDB-T was used

H.-H. Gao, Y. Sun, Dr. X. Wan, X. Ke, H. Feng, B. Kan, Y. Wang, Y. Zhang, Prof. C. Li, Prof. Y. Chen
State Key Laboratory and Institute of Elemento-Organic Chemistry
Centre of Nanoscale Science and Technology and Key Laboratory of Functional Polymer Materials
College of Chemistry
Nankai University
Tianjin 300071, China
E-mail: xjwan@nankai.edu.cn; yschen99@nankai.edu.cn

 The ORCID identification number(s) for the author(s) of this article can be found under <https://doi.org/10.1002/adv.201800307>.

© 2018 The Authors. Published by WILEY-VCH Verlag GmbH & Co. KGaA, Weinheim. This is an open access article under the terms of the Creative Commons Attribution License, which permits use, distribution and reproduction in any medium, provided the original work is properly cited.

DOI: 10.1002/adv.201800307

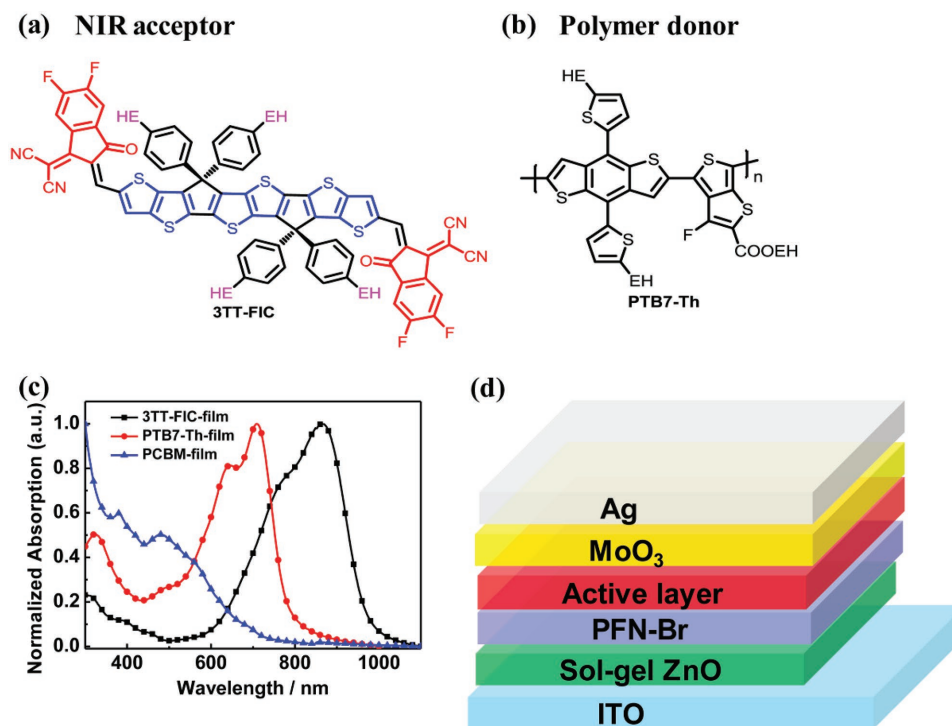


Figure 1. Chemical structures of a) **3TT-FIC** nonfullerene acceptor and b) **PTB7-Th** donor, c) UV-Vis absorption spectra of **PTB7-Th**, **PC₇₁BM**, and **3TT-FIC** in neat film, d) the device structure.

as the donor material in our case.^[34] In this work, based on the above molecule **TTIC**, we designed and synthesized a new NFA molecule **3TT-FIC** (Figure 1a) with three fused thieno[3,2-b]thiophene as the central unit flanked with two electron-withdrawing 2-(5,6-difluoro-3-oxo-2,2,3-dihydro-1H-ioden-1-ylidene)malononitrile end groups. Considering the extended conjugation framework, we choose 4-(2-ethylhexylbenzene) as the side chain to enhance its solubility. As expected, **3TT-FIC** showed maximum absorption peak located at 851 nm and a low optical bandgap of 1.25 eV. **PTB7-Th:3TT-FIC**-based devices gave a PCE of 12.21% with a high J_{sc} of 25.89 mA cm⁻². Considering the low EQE response in the range 300–500 nm for the above two-component devices, we used phenyl-C₇₁-butyric-acid-methyl ester (**PC₇₁BM**) as the third component to fabricate the ternary device in order to lift the EQE response in the range of 300–500 nm and thus improve J_{sc} without sacrificing V_{oc} and FF. As expected, an evident EQE improvement was realized in the range 300–700 nm even with a small amount of 12% **PC₇₁BM** in weight ratio. The PCE was elevated from 12.21% to 13.54% with evidently enhanced J_{sc} from 25.89 to 27.73 mA cm⁻², and also slightly improved V_{oc} and FF. From the morphology analysis, the incorporation of small amount of **PC₇₁BM** could also ameliorate the nanoscaled phase separation morphology, facilitate the charge transferring, and enhance the crystallinity in nonfullerene acceptor-based devices.

The synthetic route of **3TT-FIC** was shown in Figure S1 (Supporting Information), and the detailed synthesis procedure and the corresponding characterization data were given in the Supporting Information (SI). The precursor **1** was obtained by Stille coupling from two commercial materials and then nucleophilic addition of lithium reagent (4-(2-ethylhexylbenzene) lithium) with compound **1** to obtain the alcohol intermediate. The central unit **2** was synthesized using conc H₂SO₄ in tetrahydrofuran. The dialdehyde intermediate was prepared by the Vilsmeier–Haack reaction as a yellow-red solid. Finally, the target molecule was obtained by Knoevenagel condensation in 86% yield. As shown in the thermogravimetric analysis (Figure S2, Supporting Information) measurement, **3TT-FIC** demonstrated high thermal stability up to 340 °C without decomposition. The introduction of four 2-ethylhexyl in the side chains made **3TT-FIC** to have good solubility in chloroform, chlorobenzene, tetrahydrofuran, and other common solvents.

As shown in Figure S3 (Supporting Information), in dilute chloroform, **3TT-FIC** shows broad and strong absorption with the λ_{max} located at 799 nm ($\epsilon = 2.1 \times 10^5$ M⁻¹ cm⁻¹). In the neat film, **3TT-FIC** exhibits broaden and red-shifted absorption peaks located at 851 nm with the absorption edge extended to 995 nm, corresponding a low optical energy band gap (E_g^{opt}) of 1.25 eV (as shown in Table 1). The combination

Table 1. Photophysical and electrochemical parameters of **3TT-FIC**.

Comp.	λ_{max}^{sol} [nm]	λ_{max}^{film} [nm]	λ_{onset}^{film} [nm] ^{a)}	E_g^{opt} [eV] ^{a)}	HOMO [eV]	LUMO [eV]	ϵ_{max} (M ⁻¹ cm ⁻¹) ^{a)}
3TT-FIC	799	851	995	1.25	-5.42	-4.17	2.1×10^5

^{a)} $E_g^{opt} = 1240/\lambda_{onset}$ (eV).

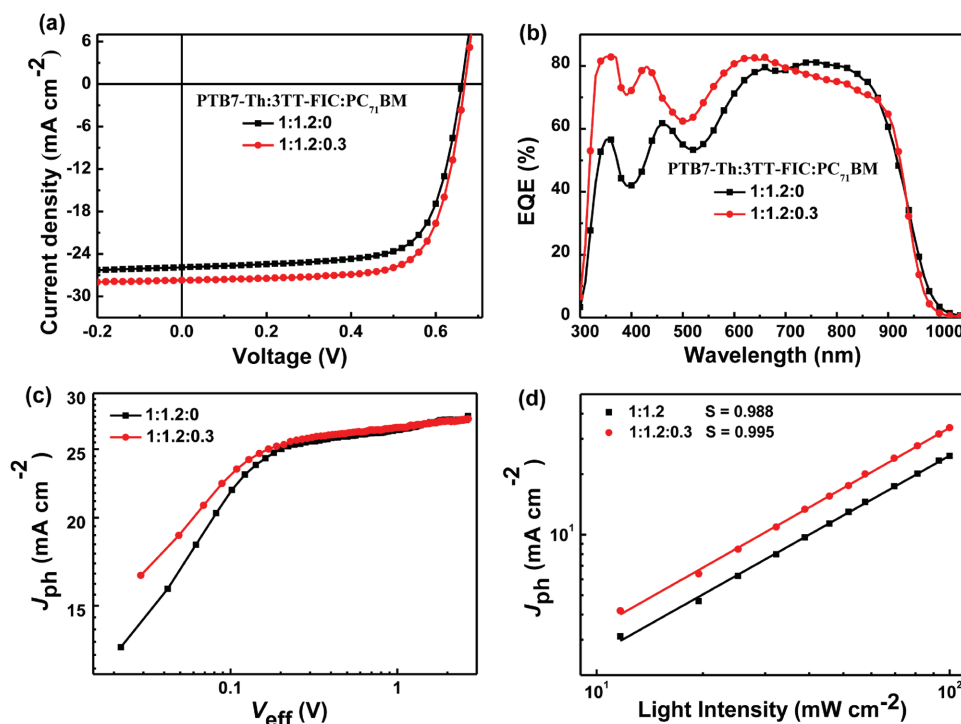


Figure 2. a) Current density–voltage (J – V) curves of PTB7-Th:3TT-FIC based binary device and PTB7-Th:3TT-FIC:PC₇₁BM based ternary device under one sun illumination (AM 1.5 G 100 mW cm^{-2}). b) EQE spectra of the corresponding devices. c) J_{ph} versus V_{eff} and d) light-intensity (P) dependence of J_{sc} measurement of the devices.

of 3TT-FIC and PTB7-Th shows broad and complementary absorption and provides a broad absorption ranging from 520 to 995 nm (Figure 1c). The density functional theory based on the B3LYP/6-31G* basis set was used to evaluate the chemical geometry structure, in which the 2-ethylhexyl side chains were replaced by methyl to simplify the calculation process. As revealed in Figure S4a (Supporting Information), the electron cloud density of highest occupied molecular orbital (HOMO) mainly located at the central building block, but its lowest unoccupied molecular orbital (LUMO) is delocalized preferably at the end group. From Figure S4b (Supporting Information), 3TT-FIC backbone shows preferable planarity with dihedral angle of 0°, which is beneficial for efficient π – π stacking and electron transfer. The HOMO/LUMO energy levels of 3TT-FIC were determined by cyclic voltammetry measurement using solid film in its acetonitrile solution (Figure S5a, Supporting Information). The HOMO and LUMO of 3TT-FIC were calculated to be -5.42 and -4.17 eV ($E_{HOMO} + E_g^{opt}$), respectively.

The OSCs devices were fabricated using an inverted structure of ITO/ZnO/PFN-Br/active layers/MoO₃/Ag, where the active layers contained the binary blend of PTB7-Th:3TT-FIC or ternary blend of PTB7-Th:3TT-FIC:PC₇₁BM. The detailed device optimization procedures were recorded in the supporting information (Tables S1 and S2, Supporting Information). For the binary devices, the optimal weight ratio of PTB7-Th:3TT-FIC was 1:1.2 (with 10 mg PTB7-Th and 12 mg 3TT-FIC dissolved in chlorobenzene) with the active layer thickness of ≈ 100 nm. A high PCE of 12.21% with J_{sc} of 25.89 mA cm^{-2} , V_{oc} of 0.662 V and a fill factor (FF) of 0.71 was achieved via a solvent vapor annealing process with chloroform. The current

density–voltage (J – V) curves of the optimized device are shown in Figure 2a, and the corresponding photovoltaic parameters are summarized in Table 2. As shown in Figure 2b, the binary OSCs gave a broad EQE response in the range from 300 to 1000 nm with high EQE values around 0.80 in the range from 660 to 820 nm. The calculated integrated J_{sc} value from EQE curve was 24.64 mA cm^{-2} , which is consistent with the measured value (25.89 mA cm^{-2}) with a mismatch of 4.8%.

Note from Figure 2b, the EQE response in the short wavelength range is clearly lower than that in the longer wavelength range. Although with overall weak absorption, PC₇₁BM has relatively good absorption and could enhance EQE response in the short wavelength range in both binary and ternary devices.^[28,29,32] Also for the ternary devices, PC₇₁BM could form cascade energy level to facilitate the charge separation and tune the active layer morphology.^[25,32,36] Thus, in order to lift the short wavelength range EQE and thus improve the J_{sc} , we chose PC₇₁BM as the third component to fabricate the PTB7-Th:3TT-FIC:PC₇₁BM

Table 2. The photovoltaic data of the optimized devices based on PTB7-Th:3TT-FIC and PTB7-Th:3TT-FIC:PC₇₁BM under the illumination of AM 1.5G (100 mW cm^{-2}).

Comp.	V_{oc} [V]	FF	J_{sc}^{J-V} [mA cm^{-2}]	PCE [%] ^{a)}
1:1.2:0	0.662	0.712	25.89	12.21 (11.96 \pm 0.25)
1:1.2:0.15	0.666	0.719	27.36	13.10 (12.79 \pm 0.31)
1:1.2:0.30	0.669	0.730	27.73	13.54 (13.33 \pm 0.21)
1:1.2:0.45	0.671	0.690	27.29	12.63 (12.28 \pm 0.35)

^{a)}The PCE values were calculated from 20 devices for each case.

ternary blend device. After carefully device optimizations, the best weight ratio of PTB7-Th: 3TT-FIC: PC₇₁BM was 1:1.2:0.3 in wt% (with 3 mg PC₇₁BM added into the binary device), and a high PCE of 13.54% with an enhanced J_{sc} of 27.73 mA cm⁻², FF of 0.73 and V_{oc} of 0.669 V was achieved. In comparison with the binary device, the ternary OSCs showed an evidently enhanced EQE response from 300 to 700 nm after incorporation of PC₇₁BM. Although the EQE response in the long wavelength range 750–900 nm was slightly downshifted as expected, the calculated integrated J_{sc} in the whole EQE response window of the ternary device was improved to 26.41 mA cm⁻² (mismatch factor of 4.7% compared with J_{sc} from J - V measurement), compared with that of 25.89 mA cm⁻² for the binary device.

The photocurrent (J_{ph}) versus the effective applied voltage (V_{eff}) (Figure 2c) measurements were conducted to investigate and compare the exciton dissociation and charge collection dynamics for the binary and ternary devices. The J_{ph} was calculated from the value of $J_L - J_D$, where J_L and J_D represent the current density under illumination and in the dark. The V_{eff} is determined by the $V_0 - V_a$, where V_0 is the voltage when $J_L = J_D$ and V_a is the applied voltage.^[37,38] As depicted in Figure 3, when V_{eff} exceeds 1.6 V, J_{ph} becomes saturated (J_{sat}), indicating both types of the devices derived high charge extraction probability under high voltages. The ratio of J_{ph}/J_{sat} calculated from the ternary device was 0.96, which is higher than that of the binary device (0.94) under short circuit conditions. In addition, under maximal

power output conditions, the ternary devices also gave a higher value (0.85) of J_{ph}/J_{sat} than that (0.83) of the binary devices. These results indicate that the addition of PC₇₁BM in the PTB7-Th:3TT-FIC based device offers higher exciton dissociation and more efficient charge collection efficiency. The light-intensity dependence of J_{sc} results are shown in Figure 2d. According to the equation of $J_{sc} \propto P^\alpha$,^[37] a slope of 0.995 and 0.988 were obtained for the ternary and binary based devices, respectively, indicating that both the ternary and binary devices showed low bimolecular recombination with the slope value close to 1. The space charge limit current measurement was used to measure the charge mobility and the corresponding curves are listed in Figure S6 a,b (Supporting Information). The electron and hole mobility of the ternary device are 2.28×10^{-4} and 2.16×10^{-4} cm² V⁻¹ s⁻¹, respectively, which are slightly larger and more balanced than those of the binary device (1.67×10^{-4} and 2.09×10^{-4} cm² V⁻¹ s⁻¹). These results are consistent with the improved FFs of the ternary devices.

The atomic force microscopy (AFM) under tapping-mode and transmission electron microscopy (TEM) were utilized to study the morphologies of the PTB7-Th:3TT-FIC blend film and also the corresponding ternary film. As shown in AFM images (Figure 3a,b), the morphology of the binary and ternary blend films showed little difference with nearly the same root-mean-square surface roughness values of 1.60 and 1.59 nm. In TEM images (Figure 3c,d), both the binary and ternary blend

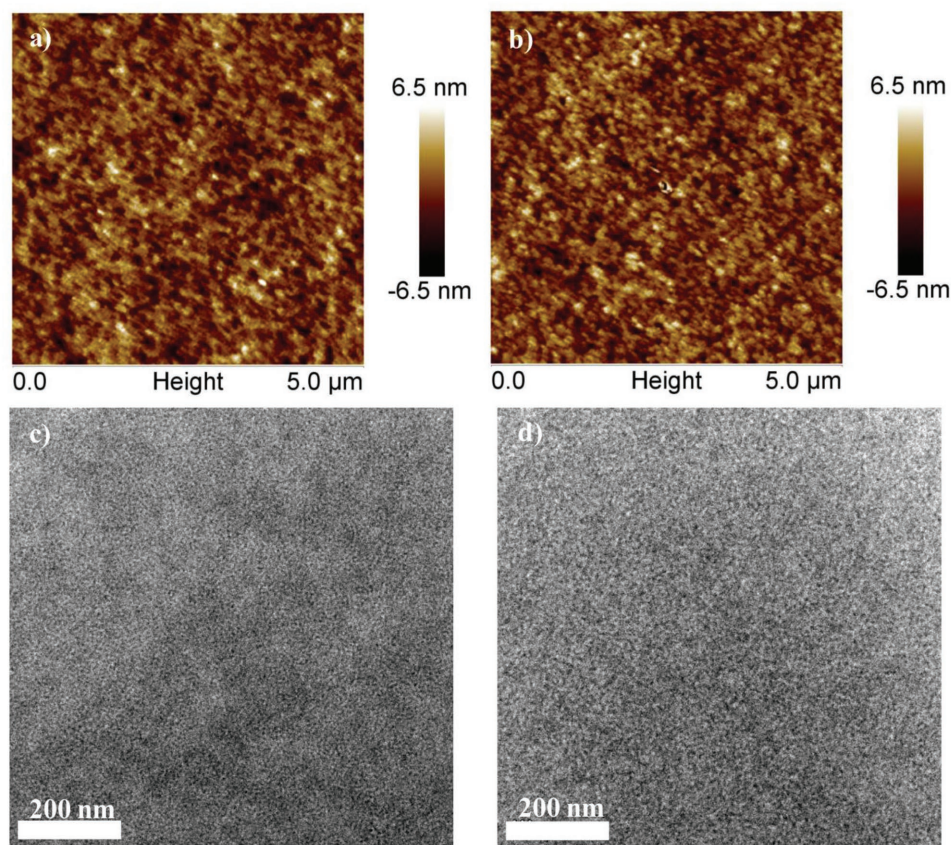


Figure 3. AFM images for a) PTB7-Th:3TT-FIC blend film and b) PTB7-Th:3TT-FIC:PC₇₁BM blend film. TEM images for c) PTB7-Th:3TT-FIC blend film and d) PTB7-Th:3TT-FIC:PCBM blend film.

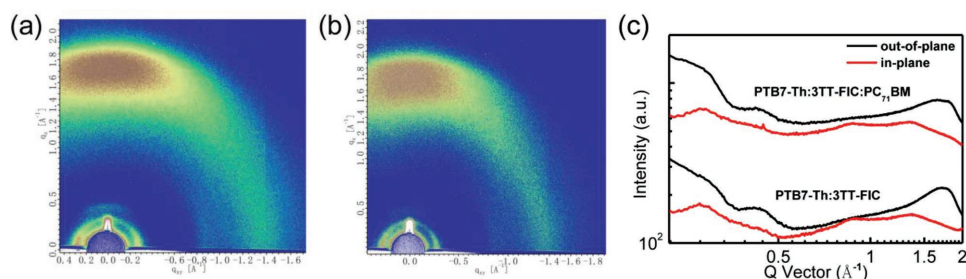


Figure 4. 2D GIXD images of the a) binary and b) ternary blend films. c) The out-of-plane (black line) and in-plane (red line) line-cut profiles.

film showed good nanoscale fibrillar structure phase separation, with the ternary based film showing relatively clearer and better continuous phase separation. The 2D grazing incidence wide-angle X-ray diffraction (GIXD) was measured to investigate the microstructural molecular packing in the blend of PTB7-Th:3TT-FIC and PTB7-Th:3TT-FIC:PC₇₁BM films (Figure 4a,b). The single component GIXD results are shown in Figure S7 (Supporting Information), where PTB7-Th polymer shows a dominant face-on orientation with a (100) reflection of 0.27 Å⁻¹ at the in-plane (IP) direction and a sharp (010) reflection at the out-of-plane (OOP) direction of 1.58 Å⁻¹. The 3TT-FIC acceptor shows a wide (100) reflection at 0.35 Å⁻¹ and a π - π stacking in the OOP direction at 1.80 Å⁻¹. The diffraction peak of PC₇₁BM located at 1.32 Å⁻¹ both in the IP and OOP direction.^[24,25] However, there was no evident PC₇₁BM diffraction peak in the ternary blend film owing to the minor addition of PC₇₁BM. From the line-cut profiles (Figure 4c), the binary and ternary blend films exhibit relatively weak (100) diffraction peaks in both the in-plane and out-of-plane directions. The binary blend film has strong (010) diffraction peaks in the out-of-plane direction, due to the combined diffraction features of PTB7-Th and 3TT-FIC and located at 1.66 Å⁻¹ and 1.81 Å⁻¹ by Gaussian fitting with the full-width at half-maximum (Δq) 0.40 and 0.23 Å, respectively (Figure S8a, Supporting Information).^[33] From Scherrer equation,^[39] the crystal coherence length (CCL) in the (010) diffraction direction was estimated to be 24.6 Å for 3TT-FIC with a π - π stacking distance of 3.47 Å. In the ternary film, contrary to the binary blend film, the (010) peak of 3TT-FIC was located at 1.83 Å⁻¹ with a Δq of 0.16 Å, which corresponds with an enhanced CCL of 34.4 Å and a shorter π - π stacking distance of 3.43 Å for 3TT-FIC (Figure S8b, Supporting Information). For the PTB7-Th, in the ternary blend film, the (010) direction located at 1.67 Å⁻¹ with a Δq of 0.40 Å, which represents a similar (010) diffraction peak and crystallinity with the binary blend film. These results indicate that the incorporation of PC₇₁BM have increased the crystallinity of 3TT-FIC and its π - π stacking pattern in the ternary device. This is consistent with the measured charge mobility and the FF values discussed above.

In summary, a new NFA named 3TT-FIC has been designed and synthesized with an extending conjugated central core and electron-withdrawing difluoro substituted indanone end group. 3TT-FIC possessed strong and broad absorption with the maximum absorption peak located at 995 nm and a low optical bandgap of 1.25 eV in the thin film. The binary device based on 3TT-FIC and PTB7-Th gave a power conversion efficiency of 12.21% with a high J_{sc} of 25.89 mA cm⁻². From the perspective

of complementary absorption and EQE response improvement, a ternary device based on the above binary OSC by introducing PC₇₁BM as the third component was fabricated and studied. A high PCE with value of 13.54% and J_{sc} of 27.73 mA cm⁻² was achieved for the ternary device. The PCE enhancement was mainly ascribed to the improved EQE response in the visible range and thus J_{sc} after the addition of PC₇₁BM. Meanwhile, the V_{oc} nearly kept unchanged and FF was also slightly improved owing to the more balanced hole and electron mobilities and better morphology with the introduction of PC₇₁BM. This work demonstrates that when the additional component was chosen properly, higher performance could be further obtained above the corresponding optimized binary devices.

Supporting Information

Supporting Information is available from the Wiley Online Library or from the author.

Acknowledgements

H.G. and Y.S. contributed equally to this work. The authors gratefully acknowledge the financial support from National Natural Science Foundation of China (NSFC) (51773095, 91633301), the Ministry of Science and Technology of China (2014CB643502) and Tianjin City (17JCJC44500, 17JCZD31100), 111 Project (B12015). The authors also thank beam line BL14B1 (Shanghai Synchrotron Radiation Facility) for providing the beam time.

Conflict of Interest

The authors declare no conflict of interest.

Keywords

nonfullerene acceptors, organic solar cells, ternary blends

Received: February 24, 2018
Published online: March 25, 2018

- [1] F. Liu, Z. Zhou, C. Zhang, J. Zhang, Q. Hu, T. Vergote, F. Liu, T. P. Russell, X. Zhu, *Adv. Mater.* **2017**, *29*, 1606574.
- [2] W. Wang, C. Yan, T. K. Lau, J. Wang, K. Liu, Y. Fan, X. Lu, X. Zhan, *Adv. Mater.* **2017**, *29*, 1701308.

- [3] Y. Li, G. Xu, C. Cui, Y. Li, *Adv. Energy Mater.* **2017**, 8, 1701791.
- [4] M. Kaltenbrunner, M. S. White, E. D. Glowacki, T. Sekitani, T. Someya, N. S. Sariciftci, S. Bauer, *Nat. Commun.* **2012**, 3, 770.
- [5] T. Kim, J. H. Kim, T. E. Kang, C. Lee, H. Kang, M. Shin, C. Wang, B. Ma, U. Jeong, T. S. Kim, B. J. Kim, *Nat. Commun.* **2015**, 6, 8547.
- [6] Z. Zhang, Z. Yang, J. Deng, Y. Zhang, G. Guan, H. Peng, *Small* **2015**, 11, 675.
- [7] W. Zhao, S. Li, H. Yao, S. Zhang, Y. Zhang, B. Yang, J. Hou, *J. Am. Chem. Soc.* **2017**, 139, 7148.
- [8] Z. Xiao, X. Jia, D. Li, S. Wang, X. Geng, F. Liu, J. Chen, S. Yang, T. P. Russell, L. Ding, *Sci. Bull.* **2017**, 62, 1494.
- [9] J. Zhu, Z. Ke, Q. Zhang, J. Wang, S. Dai, Y. Wu, Y. Xu, Y. Lin, W. Ma, W. You, X. Zhan, *Adv. Mater.* **2017**, 30, 1704713.
- [10] S. J. Xu, Z. Zhou, W. Liu, Z. Zhang, F. Liu, H. Yan, X. Zhu, *Adv. Mater.* **2017**, 29, 1704510.
- [11] B. Kan, J. Zhang, F. Liu, X. Wan, C. Li, X. Ke, Y. Wang, H. Feng, Y. Zhang, G. Long, R. H. Friend, A. A. Bakulin, Y. Chen, *Adv. Mater.* **2017**, 30, 1704904.
- [12] L. Lu, T. Zheng, Q. Wu, A. M. Schneider, D. Zhao, L. Yu, *Chem. Rev.* **2015**, 115, 12666.
- [13] O. Ostroverkhova, *Chem. Rev.* **2016**, 116, 13279.
- [14] Y. Jin, Z. Chen, S. Dong, N. Zheng, L. Ying, X. F. Jiang, F. Liu, F. Huang, Y. Cao, *Adv. Mater.* **2016**, 28, 9811.
- [15] Y. Cui, C. Yang, H. Yao, J. Zhu, Y. Wang, G. Jia, F. Gao, J. Hou, *Adv. Mater.* **2017**, 29, 1703080.
- [16] Y. Lin, J. Wang, Z. G. Zhang, H. Bai, Y. Li, D. Zhu, X. Zhan, *Adv. Mater.* **2015**, 27, 1170.
- [17] F. Zhao, S. Dai, Y. Wu, Q. Zhang, J. Wang, L. Jiang, Q. Ling, Z. Wei, W. Ma, W. You, C. Wang, X. Zhan, *Adv. Mater.* **2017**, 29, 1700144.
- [18] Y. Cui, H. Yao, B. Gao, Y. Qin, S. Zhang, B. Yang, C. He, B. Xu, J. Hou, *J. Am. Chem. Soc.* **2017**, 139, 7302.
- [19] B. Chen, X. Zheng, Y. Bai, N. P. Padture, J. Huang, *Adv. Energy Mater.* **2017**, 7, 1602400.
- [20] L. Zuo, J. Yu, X. Shi, F. Lin, W. Tang, A. K. Jen, *Adv. Mater.* **2017**, 29, 1702547.
- [21] H. Lu, X. Xu, Z. Bo, *Sci. China Mater.* **2016**, 59, 444.
- [22] Z. Xiao, X. Jia, L. Ding, *Sci. Bull.* **2017**, 62, 1562.
- [23] L. Lu, W. Chen, T. Xu, L. Yu, *Nat. Commun.* **2015**, 6, 7327.
- [24] G. Zhang, K. Zhang, Q. Yin, X.-F. Jiang, Z. Wang, J. Xin, W. Ma, H. Yan, F. Huang, Y. Cao, *J. Am. Chem. Soc.* **2017**, 139, 2387.
- [25] H. Lu, J. Zhang, J. Chen, Q. Liu, X. Gong, S. Feng, X. Xu, W. Ma, Z. Bo, *Adv. Mater.* **2016**, 28, 9559.
- [26] T. Liu, Y. Guo, Y. Yi, L. Huo, X. Xue, X. Sun, H. Fu, W. Xiong, D. Meng, Z. Wang, F. Liu, T. P. Russell, Y. Sun, *Adv. Mater.* **2016**, 28, 10008.
- [27] S. L. Chang, F. Y. Cao, W. C. Huang, P. K. Huang, C. S. Hsu, Y. J. Cheng, *ACS Appl. Mater. Interfaces* **2017**, 9, 24797.
- [28] T. H. Lee, M. A. Uddin, C. Zhong, S.-J. Ko, B. Walker, T. Kim, Y. J. Yoon, S. Y. Park, A. J. Heeger, H. Y. Woo, J. Y. Kim, *Adv. Energy Mater.* **2016**, 6, 1600637.
- [29] T. Liu, X. Xue, L. Huo, X. Sun, Q. An, F. Zhang, T. P. Russell, F. Liu, Y. Sun, *Chem. Mater.* **2017**, 29, 2914.
- [30] X. Du, X. Jiao, S. Rechberger, J. D. Perea, M. Meyer, N. Kazerouni, E. Spiecker, H. Ade, C. J. Brabec, R. H. Fink, T. Ameri, *Macromolecules* **2017**, 50, 2415.
- [31] X. Xu, Z. Bi, W. Ma, Z. Wang, W. C. H. Choy, W. Wu, G. Zhang, Y. Li, Q. Peng, *Adv. Mater.* **2017**, 29, 1704271.
- [32] Y. Zhang, D. Deng, K. Lu, J. Zhang, B. Xia, Y. Zhao, J. Fang, Z. Wei, *Adv. Mater.* **2015**, 27, 1071.
- [33] J. Zhang, Y. Zhang, J. Fang, K. Lu, Z. Wang, W. Ma, Z. Wei, *J. Am. Chem. Soc.* **2015**, 137, 8176.
- [34] H.-H. Gao, Y. Sun, X. Wan, B. Kan, X. Ke, H. Zhang, C. Li, Y. Chen, *Sci. China Mater.* **2017**, 60, 819.
- [35] X. Shi, L. Zuo, S. B. Jo, K. Gao, F. Lin, F. Liu, A. K. Y. Jen, *Chem. Mater.* **2017**, 29, 8369.
- [36] M. Zhang, J. Wang, F. Zhang, Y. Mi, Q. An, W. Wang, X. Ma, J. Zhang, X. Liu, *Nano Energy* **2017**, 39, 571.
- [37] C. M. Proctor, M. Kuik, T.-Q. Nguyen, *Prog. Polym. Sci.* **2013**, 38, 1941.
- [38] P. W. M. Blom, V. D. Mihailetschi, L. J. A. Koster, D. E. Markov, *Adv. Mater.* **2007**, 19, 1551.
- [39] D.-M. Smilgies, *J. Appl. Crystallogr.* **2009**, 42, 1030.